

# Adaptive Fractional-Order Nonsingular Fast Terminal Sliding Mode-Based Robust Tracking Control of Quadrotor UAV With Gaussian Random Disturbances and Uncertainties

Moussa LABBADI, *Student Member, IEEE*, Mohamed CHERKAOUI

**Abstract**—Random external disturbances/parametric uncertainties and other factors deteriorate the tracking control performances of the quadrotor UAV (QUAV). To achieve fast speed and high accuracy performances for the QUAV, an adaptive fractional-order nonsingular fast terminal sliding mode (AFONFTSM) controller is proposed in this paper. Nonsingular fast terminal sliding mode surfaces with fractional derivative and integral are designed for both attitude and position of the QUAV. The proposed FO nonlinear sliding surfaces ultimately and successively allow attitude and position tracking errors to converge towards zero in a finite-time. Moreover, by designing adaptive laws based on only velocity and position variables for the AFONFTSM controller, the upper bound of uncertainties/disturbances affected the QUAV dynamics are rejected. To prove the finite time convergence and zero attitude/position tracking errors using the suggested AFONFTSMC scheme, stability analysis is proposed. Simulation results under different cases show the effectiveness of the AFONFTSMC in terms of disturbances rejection and path following performances in comparison with recently FO controller, adaptive nonsingular fast terminal SMC, and other nonlinear controllers for the QUAV.

**Index Terms**—Quadrotor UAV, Finite Time Control, Nonsingular Fast Terminal Sliding Mode Control, Fractional-order, Adaptive law design, Random disturbances/uncertainties, Robust stabilization.

## I. INTRODUCTION

### A. Background and motivations

QUADROTORs, unlike conventional helicopters, can offer many attractive features, such as a variety of sizes with low weights, capable of vertical take-landing/off [1], simplicity of operation, high maneuverability, and low cost. They have been used in various fields [1], including precision agriculture, environmental monitoring, city surveillance, health, payload transportation [2], search, and rescue. Also, the QUAV is often used as the relay in wireless communications [3].

Recently, the path following control problem for the QUAV has received considerable attention in the research works. However, due to the underactuated horizontal position, nonlinearities, high couplings between the attitude and position of the QUAV, and strong external disturbances/parametric uncertainties in the dynamics of the QUAV, the controller design

M. LABBADI, and M. CHERKAOUI are with Engineering for Smart and Sustainable Systems Research Center, Mohammadia School of Engineers, Mohammed V University in Rabat, Morocco (e-mail: moussalabadi@research.emi.ac.ma).

for the QUAV system remains a significant and difficult task [4]. Therefore, external random/time-varying disturbances and random parametric uncertainties affect negatively the QUAV system control performance. To address these problems, many control techniques have been reported for the QUAV in the literature, e.g., disturbance rejection approach [35], proportional derivative and self-tuning regulator [6], backstepping [7], backpropagating constraints-based path following control [8], hierarchical control approach [19],  $H_\infty$ -based control [12], flatness-based path planning [13], and nonlinear multiple integrator [14].

One of the suitable controllers for the QUAV system control is the sliding mode control (SMC) due to its characteristics such as high precision and insensitivity to the internal/external perturbations. The terminal SMC [15] was investigated for the QUAV, in which many advantages can be obtained, including finite time convergence of QUAV states, fast convergence due to nonlinear surfaces, and insensitive to disturbances/uncertainties. However, the TSMC technique suffers from the problem of singularity. In order to solve this problem, nonsingular fast (NFTSMC) algorithms are recently developed [16], [26]. The NFTSMC method has been proposed in the literature for many control systems to improve fast speed of the variable states, finite time convergence, and to increase the system's robustness against perturbations. Compared to other SM manifolds, the NFTSMC has the capacity to reduce the control chattering and to avoid the singularity in TSMC. The fractional-order (FO) calculus is well known in the control field as an effective tool and offers two more degrees of freedom compared to integer-order. Combined FO with NFTSMC many advantages can be obtained such as strong robustness with respect to parameter variation and external disturbances, fast speed of the states, singularity avoidance, fast convergence due to the existence of the fractional derivative, and integral in the sliding surfaces. Also, by using the adaptive FONFTSMC, the estimation of the upper bounds of the disturbances/uncertainties is introduced. In this vein, the FO based on SMC has been proposed in various applications including adaptive fuzzy fractional-order SMC for permanent magnet linear synchronous motors [18], adaptive FONFTSMC for robot manipulators [19], FO fuzzy SMC for the deployment of tethered satellite system [21], adaptive super-twisting FONFTSMC for cable-driven manipulators [22].

### B. Related work

Various good related works using robust control methods for the QUAV subjected to disturbances/parametric uncertainties are recently proposed in the literature. In [23], a finite time sliding mode observer is proposed to estimate the all states of the QUAV under the influence of uncertainties and disturbances. Experimental studies are presented to validate the performance of this control strategy. The authors of [24] introduce an adaptive control approach for the aircraft to obtain balanced hover performance and stable flights. This technique is based on the second-order strictly negative imaginary controller using the type-2 fuzzy self-tuning mechanism. In order to design a physically realizable controller for the tracking trajectory of the position and attitude under the continuous disturbances, a novel FO controller is proposed in [25]. In the same context of FO based on the SMC theory, a novel control scheme is proposed in [27] to guarantee local exponential tracking of the QUAV attitude sliding manifold with a finite time convergence. Similarly, the work presented in [28] deals with the attitude control problem subjected to non-differentiable disturbances such as gust winds and turbulent effects. The control strategy used is fractional-order based on novel PI nonlinear structure, which ensures the finite time of the sliding surfaces. The work developed in [29], presents an equivalent-input-disturbance combined with PID controllers for the waypoint-tracking control of the QUAV in the presence of exogenous disturbances. An optimal guaranteed cost controller is provided by [30] to address the trajectory tracking problem of the uncertain QUAV. In [31], neural networks applied in the learning-based control method to provide a robust controller for the QUAV in the presence of time-varying and coupling uncertainties. In [32], an information fusion estimation is provided for the efficient performance of a QUAV subjected to random disturbances using a gaussian information fusion control approach. In [33], an adaptive robust control method, based on neural network backstepping and anti-saturation control method, is presented to stabilize the position and attitude of QUAV in the presence of unmodeled dynamics, input saturation, and external disturbances. Note that the papers presented in [34]–[36], respectively dealt with the problem of fixed-time attitude stabilization, adaptive finite-time (FT) attitude, and global FT trajectory tracking control for QUAV. However, these proposed FT control algorithms compensate for the negative effect on the path following performance in the outdoor flights caused by uncertainties and external disturbances. In the same context of the QUAV control in the presence of unknown disturbances and model uncertainties, a prescribed performance backstepping is provided by [38] and an adaptive nonsingular terminal SMC is proposed in [39].

### C. Contributions

Motivated by the above observations and inspired by the works developed in [16], [22], [26], [40], a new adaptive FO controller is presented in this paper to solve the path-following problem of the QUAV subjected to random parameter variations and external disturbances. By utilizing the nonlinear attitude and position sliding surfaces, the fast convergence of

these sliding manifolds can be achieved. The designed SM surfaces of the QUAV system utilizing a fractional derivative and integral are developed to improve the speed of the attitude/position states. Using fractional operations, the adaptive finite-time controller based on nonsingular fast terminal SMC law is further developed, and enhances the robustness of the QUAV system in the presence of uncertainties/disturbances. Moreover, the proposed FO controller utilizing an adaptive mechanism is designed to suppress the upper bound of uncertainties/disturbances, which are negatively affected the QUAV trajectory tracking performance. The main contributions/difficulties of this paper are summarized as follows: (i) the dynamics of QUAV considered with more complex uncertainties/disturbances compared to existing results; (ii) the designed sliding mode surfaces for the QUAV attitude and position with the FO terms, bring great advantages on the QUAV control system such as rapid trajectory tracking performance, and fast finite-time convergence; (iii) adaptive laws utilizing only velocity and position of attitude/position as informations, are introduced to cope the upper bound of the disturbances, which gives realizable adaptive laws; (iv) the efficiency of the proposed controller is compared with the nonlinear controllers [9], [10], [37], the FO control method [17], and the finite-time control methods [26].

### D. Paper organization

The rest of this paper is structured as follows: Section II describes the main FO definitions. Section III gives the dynamical model of the QUAV. In Section IV, the proposed FO controller including the stability proof is introduced. Three simulation results compared with recent flight controllers are presented and discussed in Section V. The conclusion of this work is given in Section VI.

## II. PRELIMINARIES

In this section, some basic properties and definitions of the fractional operators most used in the literature are recalled.

**Definition 1.** The Reimann-Liouville (RL) fractional integral and derivative of order  $\gamma$  for a function  $\kappa(t)$  respectively, are given by [41], [42]:

$$_a^{RL}I_t^\gamma \kappa(t) = \frac{1}{\Gamma(\hbar)} \int_a^t \frac{\kappa(\tau)}{(t-\tau)^{1-\gamma}} d\tau \quad (1)$$

and

$$_a^{RL}D_t^\gamma \kappa(t) = \frac{1}{\Gamma(\hbar-\gamma)} \frac{d^\hbar}{dt^\hbar} \int_a^t \frac{\kappa(\tau)}{(t-\tau)^{\gamma-\hbar+1}} d\tau \quad (2)$$

**Definition 2.** The  $\gamma^{th}$ -order Caputo fractional derivative of a function  $\kappa(t)$  is given by the following equation [41], [42].

$$_a^C D_t^\gamma \kappa(t) = \frac{1}{\Gamma(\gamma-\hbar)} \int_a^t \frac{\kappa^{(\hbar)}(\tau)}{(t-\tau)^{\gamma-\hbar+1}} d\tau \quad (3)$$

where  $\hbar \in \mathbb{N}^*$ ,  $\gamma$  represents the order of the derivative such that  $(\hbar-1) < \gamma < \hbar$  and  $a$  is the terminal value of  $t$  and  $\Gamma(\cdot)$  denotes the Gamma function defined as:

$$\Gamma(h) = \int_0^\infty e^{-t} t^{h-1} dt, \quad (4)$$

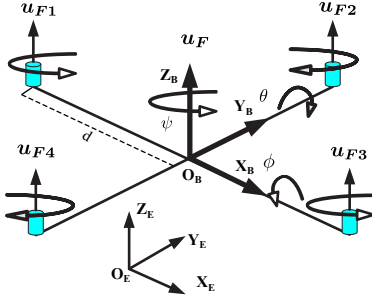


Fig. 1: Geometry of a QUAV.

## Properties.

- The identity operator of the operation  ${}_a D_t^\gamma \kappa(t)$  for  $\gamma = 0$

$$D_t^\gamma \kappa(t) = \kappa(t)$$

- Linear operations of the Fractional integration and differentiation.

$$D_t^\gamma (\alpha_1 \kappa_1(t) + \alpha_2 \kappa_2(t)) = \alpha_1 D_t^\gamma \kappa_1(t) + \alpha_2 D_t^\gamma \kappa_2(t)$$

- [43]:

$$D_t^\gamma \kappa(t) = D_{t_a}^{\gamma_1} D_{t_2}^{\gamma_2} \dots D_{t_h}^{\gamma_h} \kappa(t) \\ \gamma = \gamma_1 + \gamma_2 + \dots + \gamma_n, \gamma_i < 1, i = 1, 2, \dots, h \quad (5)$$

- The  $\gamma^{th}$ - RL FO is the left inverse of the RL fractional integral of the same order [43]:

$${}_a^{RL} D_t^\gamma I_t^\gamma \kappa(t) = \kappa(t)$$

The notation  ${}^{RL} D_t^\gamma$  used for Riemann Liouville operator will be replaced by  $D_t^\gamma$  in what follows of this paper.

Lemma 1 is used to explain the finite-time stability under fast time convergence.

**Lemma 1.** [44]: consider the Lyapunov function  $\aleph(t)$  with initial value  $\aleph_0$  is given as

$$\aleph(t) \leq -\mu_a \aleph(t) - \mu_b \aleph^\nu(t), \quad \forall t \geq t_0, \quad \aleph(t_0) \geq 0 \quad (6)$$

where,  $\mu_a > 0$ ,  $\mu_b > 0$ ,  $0 < \nu < 1$ . Let us  $\aleph(t)$ ,  $\forall t > t_1$ , hence, the settling time  $t_s$  can be obtained as

$$t_s = t_0 + \frac{1}{\mu_a(1-\nu)} \ln \frac{\mu_a \aleph^{1-\nu}(t_0) + \mu_b}{\mu_b} \quad (7)$$

## III. PROBLEM FORMULATION

The vehicle used in this paper is a mini QUAV, which has four rotors. As presented in Fig. 1, the vectors  $\mathbf{X}_p = [x \ y \ z]^T \in \mathbb{R}^3$  and  $\boldsymbol{\eta}_\varphi = [\phi \ \theta \ \psi]^T \in \mathbb{R}^3$  denote position and orientation of the QUAV respectively in the earth-fixed inertial frame  $\{\mathbf{O}_E, \mathbf{X}_E, \mathbf{Y}_E, \mathbf{Z}_E\}$ . The linear and angular velocities are denoted by  $\mathbf{v}_p = [u \ v \ w]^T$ , respectively in the body-fixed frame  $\{\mathbf{O}_B, \mathbf{X}_B, \mathbf{Y}_B, \mathbf{Z}_B\}$ . The orientation of the QUAV is presented by a rotation matrix  $\mathbf{R}$ . The Newton-Euler method gives the equations of motion of the QUAV as [16], [26]

$$m \ddot{\mathbf{X}}_p = m g e_z - \mathbf{R} \mathbf{u}_F e_z - K_p \dot{\mathbf{X}}_p + d_p(t) \quad (8a)$$

$$I \ddot{\boldsymbol{\eta}}_\varphi = \boldsymbol{\eta}_\varphi \times I \boldsymbol{\eta}_\varphi + \boldsymbol{\tau}_c + \boldsymbol{\tau} - K_\varphi \dot{\boldsymbol{\eta}}_\varphi^2 + d_{\boldsymbol{\eta}_\varphi}(t) \quad (8b)$$

where  $\mathbf{u}_F \in \mathbb{R}$  is the total thrust along the vertical axis of  $\mathbf{O}_B$  and  $\boldsymbol{\tau} = [\tau_x \ \tau_y \ \tau_z]^T$  in  $\mathbf{O}_B$  is the torque control.  $e_z = [0 \ 0 \ 1]^T$ .  $m$  is the mass of the QUAV.  $g$  is the gravitational acceleration.  $K_\varphi = \text{diag}[K_{\varphi 1}, K_{\varphi 2}, K_{\varphi 3}]$  and  $K_p = \text{diag}[K_{px}, K_{py}, K_{pz}]$  are the aerodynamic coefficient matrices.  $\boldsymbol{\tau}_c$  is the resultant torque due to the gyroscopic effect.  $d_p(t) = \text{diag}[d_{px}(t), d_{py}(t), d_{pz}(t)]$  and  $d_{\boldsymbol{\eta}_\varphi}(t) = \text{diag}[d_{\varphi 1}(t), d_{\varphi 2}(t), d_{\varphi 3}(t)]$  are external disturbances.  $I = \text{diag}[I_{11}, I_{22}, I_{33}]$  is the inertia matrix. The expression of the rotation matrix  $\mathbf{R}$  can be obtained by three successive rotations  $Z \rightarrow Y \rightarrow X$  as:

$$\mathbf{R} = \begin{bmatrix} C_\psi C_\theta & S_\psi C_\theta & -S_\theta \\ C_\psi S_\phi S_\theta - C_\phi S_\psi & S_\psi S_\phi S_\theta + C_\phi C_\psi & S_\phi C_\theta \\ C_\phi C_\psi S_\theta + S_\phi S_\psi & C_\phi S_\psi S_\theta - S_\phi C_\psi & C_\phi C_\theta \end{bmatrix}^T \quad (9)$$

The control inputs  $\boldsymbol{\tau}$  and  $\mathbf{u}_F$  can be obtained as [8]:

$$\begin{bmatrix} \mathbf{u}_F \\ \boldsymbol{\tau}_x \\ \boldsymbol{\tau}_y \\ \boldsymbol{\tau}_z \end{bmatrix} = \begin{bmatrix} \rho_b & \rho_b & \rho_b & \rho_b \\ 0 & -\rho_b d & 0 & +\rho_b d \\ -\rho_b d & 0 & \rho_b d & 0 \\ -\rho_c & \rho_c & -\rho_c & \rho_c \end{bmatrix} \begin{bmatrix} \mathbf{u}_{F1} \\ \mathbf{u}_{F2} \\ \mathbf{u}_{F3} \\ \mathbf{u}_{F4} \end{bmatrix} \quad (10)$$

where  $d$  is the distance between the rotor axis and the mass center of the QUAV.  $\rho_b$  and  $\rho_c$  are respectively the drag and thrust factors. Consider the mathematical model of a QUAV, which describes the full dynamics under external disturbances [16], [26].

$$\ddot{\phi} = a_{\phi_1} \dot{\phi} \dot{\psi} - a_{\phi_2} \dot{\phi} \varphi - a_{\phi_3} \dot{\phi}^2 + a_{\Phi_1} \boldsymbol{\tau}_x + \frac{d_{\varphi 1}(t)}{I_{11}} \quad (11a)$$

$$\ddot{\theta} = a_{\theta_1} \dot{\phi} \dot{\psi} + a_{\theta_2} \dot{\phi} \varphi - a_{\theta_3} \dot{\theta}^2 + a_{\Theta_1} \boldsymbol{\tau}_y + \frac{d_{\varphi 2}(t)}{I_{22}} \quad (11b)$$

$$\ddot{\psi} = a_{\psi_1} \dot{\phi} \dot{\theta} - a_{\psi_2} \dot{\psi}^2 + a_{\Psi_1} \boldsymbol{\tau}_z + \frac{d_{\varphi 3}(t)}{I_{33}} \quad (11c)$$

$$\ddot{x} = (C_\psi S_\theta C_\phi + S_\psi S_\phi) \frac{\mathbf{u}_F}{m} - b_x \dot{x} + \frac{d_{px}(t)}{m} \quad (11d)$$

$$\ddot{y} = (S_\psi S_\theta C_\phi - C_\psi S_\phi) \frac{\mathbf{u}_F}{m} - b_y \dot{y} + \frac{d_{py}(t)}{m} \quad (11e)$$

$$\ddot{z} = -g + C_\theta C_\phi \frac{\mathbf{u}_F}{m} - b_z \dot{z} + \frac{d_{pz}(t)}{m} \quad (11f)$$

$$a_{\phi_1} = \frac{I_{22} - I_{33}}{I_{11}}, a_{\phi_2} = \frac{J_r}{I_{11}}, a_{\phi_3} = \frac{K_{\varphi 1}}{I_{11}}, a_{\Phi_1} = \frac{1}{I_{11}}, \\ a_{\theta_1} = \frac{I_{33} - I_{11}}{I_{22}}, a_{\theta_2} = \frac{J_r}{I_{22}}, a_{\theta_3} = \frac{K_{\varphi 2}}{I_{22}}, a_{\Theta_1} = \frac{1}{I_{22}}, a_{\psi_1} = \frac{I_{11} - I_{22}}{I_{33}}, \\ a_{\psi_2} = \frac{K_{\varphi 3}}{I_{33}}, a_{\Psi_1} = \frac{1}{I_{33}}, b_x = \frac{K_{px}}{m}, b_y = \frac{K_{py}}{m}, b_z = \frac{K_{pz}}{m}.$$

where  $\varphi = \omega_1 - \omega_2 + \omega_3 - \omega_4$ .

**Assumption 1.** The Euler angles are bounded as  $\phi, \theta \in [-\frac{\pi}{2}, \frac{\pi}{2}]$ , and  $\psi \in [-\pi, \pi]$ .

**Assumption 2.** The disturbances  $d_{\boldsymbol{\eta}_\varphi}(t)$  and  $d_p(t)$  affected the dynamics of the translational and rotational are bounded respectively by  $D_{\boldsymbol{\eta}_\varphi}(t)$  and  $D_p(t)$ .

The outputs  $[x \ y \ z \ \phi \ \theta \ \psi]^T$  of the QUAV are controlled by only four signal inputs  $[\mathbf{u}_F \ \boldsymbol{\tau}_x \ \boldsymbol{\tau}_y \ \boldsymbol{\tau}_z]^T$ . Three virtual controls are introduced  $\mathbf{u}_F, \phi$  and  $\theta$  to solve the under-actuated problem of the horizontal position as follows:

$$\mathbf{v} = \begin{bmatrix} \mathbf{v}_x \\ \mathbf{v}_y \\ \mathbf{v}_z \end{bmatrix} = \begin{bmatrix} (C_\psi S_\theta C_\phi + S_\psi S_\phi) \frac{\mathbf{u}_F}{m} \\ (S_\psi S_\theta C_\phi - C_\psi S_\phi) \frac{\mathbf{u}_F}{m} \\ C_\theta C_\phi \frac{\mathbf{u}_F}{m} \end{bmatrix} \quad (12)$$

Then, the desired angles  $\phi^r$ ,  $\theta^r$ , and the thrust  $\mathbf{u}_F$  can be formulated as:

$$\phi^r = \arctan(C_{\theta^r} \frac{S_{\psi^r} \mathbf{v}_x - C_{\psi^r} \mathbf{v}_y}{\mathbf{v}_z + g}) \quad (13a)$$

$$\theta^r = \arctan(\frac{C_{\psi^r} \mathbf{v}_x + S_{\psi^r} \mathbf{v}_y}{\mathbf{v}_z + g}) \quad (13b)$$

$$\mathbf{u}_F = m \sqrt{\mathbf{v}_x^2 + \mathbf{v}_y^2 + (\mathbf{v}_z + g)^2} \quad (13c)$$

In this view, in the presence of both complex disturbances  $d_{\eta_\varphi}(t)$  and  $d_p(t)$ , the control objective is to design the virtual controller  $\mathbf{v} = [\mathbf{v}_x \ \mathbf{v}_y \ \mathbf{v}_z]^T$  for position loop, which generates the total lift  $\mathbf{u}_F$  and the desired  $[\phi^r \ \theta^r]^T$  angles such that the position vector  $\mathbf{X}_P = [x \ y \ z]$  tracks the desired position  $\mathbf{X}_P^r = [x^r \ y^r \ z^r]^T$ . For the attitude loop, the objective control is to design yaw  $\tau_z$ , roll  $\tau_x$ , and pitch  $\tau_y$  controllers such that the attitude vector  $\boldsymbol{\eta}_\varphi = [\phi \ \theta \ \psi]^T$  converges vers  $\boldsymbol{\eta}_\varphi^r = [\phi^r \ \theta^r \ \psi^r]^T$ .

#### IV. CONTROLLER DESIGN

In this section, an adaptive robust fractional-order controller is proposed for path-following of a QUAV under unknown random uncertainties and disturbances. Based on the properties of fractional theory and sliding mode controller with nonsingular fast terminal sliding surfaces, a new control approach is presented to attenuate the negative effect affected the QUAV dynamics. Figure 2 shows the flight control scheme proposed in this paper. The resulting controller is robust against random external disturbances and other factors, simple and easy to implement in the real time application. The design process of the flight controller is given in the following subsections for the attitude and position.

##### A. Translational subsystem

Inspired by the works presented in [26], [40] and motivated by the problems of the random parametric uncertainties of the QUAV such as drag coefficients, total mass, and moment inertial. Also, the problem of random external disturbances is considered in this work. The proposed controller for the position subsystem is based on a nonlinear terminal fast sliding mode control algorithm. To improve the tracking performances under these problems and increase the convergence speed of the state variables, two degrees of freedom like FO integral and derivative are employed with the nonlinear sliding mode surfaces for the position subsystem. In this part, the virtual controllers are designed to generate the total lift and desired tilting angles.

To achieve the above objectives, define the outer-loop tracking errors as follows:

$$\mathbf{e}_x^1 = x - x^r, \quad \mathbf{e}_y^1 = y - y^r, \quad \mathbf{e}_z^1 = z - z^r \quad (14)$$

$$\mathbf{e}_x^2 = \dot{x} - \dot{x}^r, \quad \mathbf{e}_y^2 = \dot{y} - \dot{y}^r, \quad \mathbf{e}_z^2 = \dot{z} - \dot{z}^r \quad (15)$$

Then, the FO nonsingular FTSM surfaces for the translational subsystem are given by:

$$\mathbf{S}_x^P = \mathbf{e}_x^2 + D^{\gamma_{x1}-1} c_{x1} \mathbf{e}_x^{1p_x/q_x} + I^{\gamma_{x2}} c_{x2} \mathbf{e}_x^{1\varphi_x} sgn(\mathbf{e}_x^1) \quad (16)$$

$$\mathbf{S}_y^P = \mathbf{e}_y^2 + D^{\gamma_{y1}-1} c_{y1} \mathbf{e}_y^{1p_y/q_y} + I^{\gamma_{y2}} c_{y2} \mathbf{e}_y^{1\varphi_y} sgn(\mathbf{e}_y^1) \quad (17)$$

$$\mathbf{S}_z^P = \mathbf{e}_z^2 + D^{\gamma_{z1}-1} c_{z1} \mathbf{e}_z^{1p_z/q_z} + I^{\gamma_{z2}} c_{z2} \mathbf{e}_z^{1\varphi_z} sgn(\mathbf{e}_z^1) \quad (18)$$

where  $c_{i1}$ ,  $c_{i2}$ , and  $\varphi_i$  for  $i = x, y, z$  are positive parameters. The parameters  $p_i$  and  $q_i$  satisfied that  $1 < p_i/q_i < 2$ . The fractional orders  $\gamma_{i1}$  and  $\gamma_{i2}$  are  $0 < \gamma_{i1}, \gamma_{i2} < 1$ . where  $sgn(x)$  equals 1,  $x \leq 0$  or 0,  $x < 0$ .

**Remark 1.** The singularity problem in TSM may occur if the initial conditions are not selected carefully. Therefore, it would result in an infinite control law. In fact, the proposed terminal sliding surface is rewritten as:

$$\mathbf{S}_i^P = \mathbf{e}_i^2 + D^{\gamma_{i1}-1} c_{i1} \mathbf{e}_i^{1p_i/q_i} + I^{\gamma_{i2}} c_{i2} \mathbf{e}_i^{1\varphi_i} sgn(\mathbf{e}_i^1) \quad (19)$$

if  $0.5 < p_i/q_i < 1$ . The singularity problem may occur in the TSMS (19) in this case.

In order to solve this problem, the following condition can be applied, which is known as the nonsingular TSMC. If so that if  $1 < p_i/q_i < 2$ , then when  $\mathbf{S}_i^P \rightarrow 0$ ,  $\mathbf{u}_i$  is bounded.

The dynamic of FONFTSM manifolds can be written as:

$$\dot{\mathbf{S}}_x^P = \dot{\mathbf{e}}_x^2 + D^{\gamma_{x1}} c_{x1} \mathbf{e}_x^{1p_x/q_x} + I^{\gamma_{x2}} c_{x2} \varphi_x |\mathbf{e}_x^1|^{\varphi_x-1} \mathbf{e}_x^2 \quad (20)$$

$$\dot{\mathbf{S}}_y^P = \dot{\mathbf{e}}_y^2 + D^{\gamma_{y1}} c_{y1} \mathbf{e}_y^{1p_y/q_y} + I^{\gamma_{y2}} c_{y2} \varphi_y |\mathbf{e}_y^1|^{\varphi_y-1} \mathbf{e}_y^2 \quad (21)$$

$$\dot{\mathbf{S}}_z^P = \dot{\mathbf{e}}_z^2 + D^{\gamma_{z1}} c_{z1} \mathbf{e}_z^{1p_z/q_z} + I^{\gamma_{z2}} c_{z2} \varphi_z |\mathbf{e}_z^1|^{\varphi_z-1} \mathbf{e}_z^2 \quad (22)$$

Finally, we shall give the form of the AFONFTSM controller for the position subsystem based on the fractional derivative and integral. By using (11d)-(11f), (41), and (20)-(22) and letting  $\dot{\mathbf{S}}_x^P = \dot{\mathbf{S}}_y^P = \dot{\mathbf{S}}_z^P = 0$ ;  $d_{px}(t) = d_{py}(t) = d_{pz}(t) = 0$  in (20)-(22), the equivalent control inputs for the position loop can be obtained as:

$$\mathbf{v}_{x0} = b_x \dot{x} + \ddot{x}^r - D^{\gamma_{x1}} c_{x1} \mathbf{e}_x^{1p_x/q_x} - I^{\gamma_{x2}} c_{x2} \varphi_x |\mathbf{e}_x^1|^{\varphi_x-1} \mathbf{e}_x^2$$

$$\mathbf{v}_{y0} = b_y \dot{y} + \ddot{y}^r - D^{\gamma_{y1}} c_{y1} \mathbf{e}_y^{1p_y/q_y} - I^{\gamma_{y2}} c_{y2} \varphi_y |\mathbf{e}_y^1|^{\varphi_y-1} \mathbf{e}_y^2$$

$$\mathbf{v}_{z0} = b_z \dot{z} + \ddot{z}^r - D^{\gamma_{z1}} c_{z1} \mathbf{e}_z^{1p_z/q_z} - I^{\gamma_{z2}} c_{z2} \varphi_z |\mathbf{e}_z^1|^{\varphi_z-1} \mathbf{e}_z^2 \quad (23)$$

**Assumption 3.** The external disturbances/uncertainties  $\frac{d_p(t)}{m}$  and  $\frac{d_{\eta_\varphi}(t)}{I}$  are unknown and assumed to be bounded respectively by  $D_p(t)$  and  $D_{\eta_\varphi}(t)$ , i.e.  $\frac{d_p(t)}{m} \leq D_p(t) \leq |D_p|$  and  $\frac{d_{\eta_\varphi}(t)}{I} \leq D_{\eta_\varphi}(t) \leq |D_{\eta_\varphi}|$ .

We suppose that the upper bounds  $D_p(t)$  and  $D_{\eta_\varphi}(t)$  contain only the tracking errors and its derivatives such as:  $|D_p| = b_{0k} + b_{1k} \mathbf{e}_j^1 + b_{2k} \mathbf{e}_j^2$  and  $|D_{\eta_\varphi}| = b_0 + b_1 \mathbf{e}_j^1 + b_2 \mathbf{e}_j^2$ , for  $i = x, y, z$ ,  $j = \phi, \theta, \psi$ , and  $k = 1, 3, 5, 7, 9, 11$ .

In order to ensure good tracking accuracy with the existence of the unknown random disturbance/uncertainty and to guarantee fast convergence of translational states, the reaching control inputs are designed as:

$$\begin{aligned} \mathbf{v}_{x1} &= -\hbar_{x1} sgn(\mathbf{S}_x^P) - \hbar_{x2} \mathbf{S}_x^P - (\hat{b}_{07} + \hat{b}_{17} \mathbf{e}_x^1 + \hat{b}_{27} \mathbf{e}_x^2 + \mu) sgn(\mathbf{S}_x^P) \\ \mathbf{v}_{y1} &= -\hbar_{y1} sgn(\mathbf{S}_y^P) - \hbar_{y2} \mathbf{S}_y^P - (\hat{b}_{09} + \hat{b}_{19} \mathbf{e}_y^1 + \hat{b}_{29} \mathbf{e}_y^2 + \mu) sgn(\mathbf{S}_y^P) \\ \mathbf{v}_{z1} &= -\hbar_{z1} sgn(\mathbf{S}_z^P) - \hbar_{z2} \mathbf{S}_z^P - (\hat{b}_{011} + \hat{b}_{111} \mathbf{e}_z^1 + \hat{b}_{211} \mathbf{e}_z^2 + \mu) sgn(\mathbf{S}_z^P) \end{aligned} \quad (24)$$

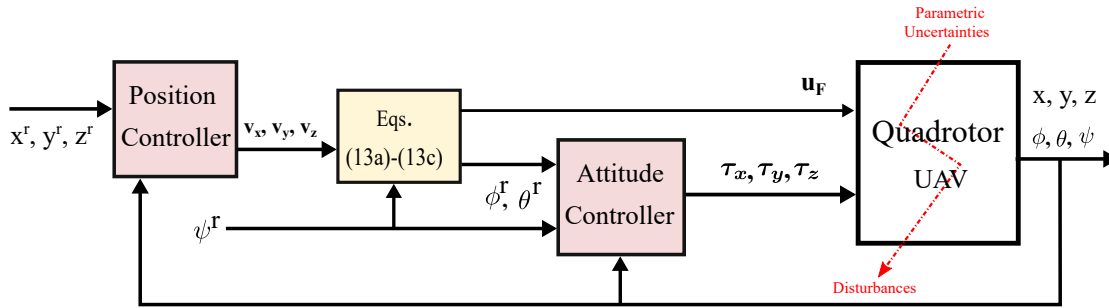


Fig. 2: The AFONFTSMC scheme for QUAV.

where  $\hbar_{i1}$  and  $\hbar_{i2}$  are the control parameters, and  $\mu$  is a smaller parameter; and  $\hat{b}_{0k}$ ,  $\hat{b}_{1k}$ , and  $\hat{b}_{2k}$  for  $k = 7, 9, 11$  are updated by the adaptive laws formulated as:

$$\dot{\hat{b}}_{07} = \eta_{x0} |\mathbf{S}_x^P|, \quad \dot{\hat{b}}_{17} = \eta_{x1} \mathbf{e}_x^1 |\mathbf{S}_x^P|, \quad \dot{\hat{b}}_{27} = \eta_{x2} \mathbf{e}_x^2 |\mathbf{S}_x^P| \quad (25)$$

$$\dot{\hat{b}}_{09} = \eta_{y0} |\mathbf{S}_y^P|, \quad \dot{\hat{b}}_{19} = \eta_{y1} \mathbf{e}_y^1 |\mathbf{S}_y^P|, \quad \dot{\hat{b}}_{29} = \eta_{y2} \mathbf{e}_y^2 |\mathbf{S}_y^P| \quad (26)$$

$$\dot{\hat{b}}_{011} = \eta_{z0} |\mathbf{S}_z^P|, \quad \dot{\hat{b}}_{111} = \eta_{z1} \mathbf{e}_z^1 |\mathbf{S}_z^P|, \quad \dot{\hat{b}}_{211} = \eta_{z2} \mathbf{e}_z^2 |\mathbf{S}_z^P| \quad (27)$$

where  $\eta_{i0}$ ,  $\eta_{i1}$ , and  $\eta_{i2}$  for  $i = x, y, z$  to be designed. Hence, the overall virtual controllers obtained via the AFONFTSMC can be given by:

$$\mathbf{v}_x = \mathbf{v}_{x0} + \mathbf{v}_{x1}, \quad \mathbf{v}_y = \mathbf{v}_{y0} + \mathbf{v}_{y1}, \quad \mathbf{v}_z = \mathbf{v}_{z0} + \mathbf{v}_{z1} \quad (28)$$

with  $\mathbf{v}_{x0}$ ,  $\mathbf{v}_{x1}$ ,  $\mathbf{v}_{y0}$ ,  $\mathbf{v}_{y1}$ ,  $\mathbf{v}_{z0}$ , and  $\mathbf{v}_{z1}$  given by (23) and (24).

### B. Stability Analysis for the translational loop

The performance of the ANFTSMC for the position-loop is summarized and explained in Theorems 1 and 2. Also, the stability analysis is provided for the translational subsystem.

**Theorem 1.** Consider the  $x$ -subsystem control problem of the QUAV (11d) under disturbances with Assumption 3. Design the AFONFTSMC approach in (24) and their adaptation laws in (25), then, the both tracking errors converge to zero in a finite time.

*Proof.* First, the adaptive estimation errors can be defined as:  $\tilde{b}_{07} = \hat{b}_{07} - b_{07}$ ,  $\tilde{b}_{17} = \hat{b}_{17} - b_{17}$ , and  $\tilde{b}_{27} = \hat{b}_{27} - b_{27}$ . Assuming the time-derivative of estimation errors as:  $\dot{\tilde{b}}_{07} = \hat{\dot{b}}_{07}$ ,  $\dot{\tilde{b}}_{17} = \hat{\dot{b}}_{17}$ , and  $\dot{\tilde{b}}_{27} = \hat{\dot{b}}_{27}$ .

Next, define the Lyapunov function  $V_x^p$  as

$$V_x^p = \frac{1}{2} \mathbf{S}_x^P \mathbf{S}_x^P + \sum_{i=1}^2 \frac{1}{2\eta_{xi}} \tilde{b}_{i7}^2, \quad i = 1, 2, 3 \quad (29)$$

with  $\eta_{xi}$  is a positive number. Using the time-derivative of  $\mathbf{S}_x^P$  defined in (16) and using the AFONFTSMC in (28), the

time-derivative of  $V_x^p$  can be written as

$$\begin{aligned} \dot{V}_x^p &= \mathbf{S}_x^P \dot{\mathbf{S}}_x^P + \sum_{i=1}^2 \frac{1}{\eta_{xi}} \tilde{b}_{i7} \dot{\tilde{b}}_{i7} \\ &= \mathbf{S}_x^P \{ \mathbf{v}_{x1} - b_x \dot{x} + \frac{d_{px}(t)}{m} - \ddot{x}^r + D^{\gamma_{x1}} c_{x1} \mathbf{e}_x^1 p_x / q_x \\ &\quad + I^{\gamma_{x2}} c_{x2} \varphi_x |\mathbf{e}_x^1|^{\varphi_x-1} \mathbf{e}_x^2 \} + \sum_{i=1}^2 \frac{1}{\eta_{xi}} \tilde{b}_{i7} \dot{\tilde{b}}_{i7} \\ &= \mathbf{S}_x^P \{ -\hbar_{x1} sgn(\mathbf{S}_x^P) - \hbar_{x2} \mathbf{S}_x^P - (\hat{b}_{07} + \hat{b}_{17} \mathbf{e}_x^1 + \hat{b}_{27} \mathbf{e}_x^2 \\ &\quad + \mu) sgn(\mathbf{S}_x^P) + \frac{d_{px}(t)}{m} \} + \sum_{i=1}^2 \frac{1}{\eta_{xi}} \tilde{b}_{i7} \dot{\tilde{b}}_{i7} \\ &\leq -\hbar_{x1} |\mathbf{S}_x^P| - \hbar_{x2} \mathbf{S}_x^P \mathbf{S}_x^P - (\hat{b}_{07} + \hat{b}_{17} \mathbf{e}_x^1 + \hat{b}_{27} \mathbf{e}_x^2) |\mathbf{S}_x^P| \\ &\quad + |D_{px}| \mathbf{S}_x^P + \sum_{i=1}^2 \frac{1}{\eta_{xi}} \tilde{b}_{i7} \dot{\tilde{b}}_{i7} \\ &\leq -(\hbar_{x1} + \mu) |\mathbf{S}_x^P| - \hbar_{x2} \mathbf{S}_x^P \mathbf{S}_x^P - (\hat{b}_{07} + \hat{b}_{17} \mathbf{e}_x^1 + \hat{b}_{27} \mathbf{e}_x^2) |\mathbf{S}_x^P| \\ &\quad + (b_{07} + b_{17} \mathbf{e}_z^1 + b_{27} \mathbf{e}_z^2) |\mathbf{S}_x^P| + \frac{1}{\eta_{x0}} (\hat{b}_{07} - b_{07}) \dot{\hat{b}}_{07} \\ &\quad + \frac{1}{\eta_{x1}} (\hat{b}_{17} - b_{17}) \dot{\hat{b}}_{17} + \frac{1}{\eta_{x2}} (\hat{b}_{27} - b_{27}) \dot{\hat{b}}_{27} \end{aligned} \quad (30)$$

By replacing the adaptive laws (25) in (30), it yields

$$\dot{V}_x^p \leq -(\hbar_{x1} + \mu) |\mathbf{S}_x^P| - \hbar_{x2} \mathbf{S}_x^P \mathbf{S}_x^P \quad (31)$$

The differential inequality can be rewritten as:

$$\dot{V}_x^p \leq -\sqrt{2}(\hbar_{x1} + \mu)V_x^{p0.5} - 2\hbar_{x2}V_x^p \quad (32)$$

Define  $\lambda_{x1} = \sqrt{2}(\hbar_{x1} + \mu)$  and  $\lambda_{x2} = 2\hbar_{x2}$ . The differential inequality can be presented in the same form as that in Lemma 1, it yields

$$\dot{V}_x^p \leq -\lambda_{x1} V_x^{p0.5} - \lambda_{x2} V_x^p \quad (33)$$

From above differential inequality, it can be confirmed that both tracking errors of  $x$ -subsystem will reach the sliding mode in a finite time  $t_x^p$  given by:

$$t_x^p \leq t_{x0} + \frac{2}{\lambda_{x1}} \ln \left( \frac{\lambda_{x1} V_x^{p0.5}(t_{x0}) + \lambda_{x2}}{\lambda_{x2}} \right) \quad (34)$$

Hence, the finite-time stability of the  $x$ -subsystem is obtained.  $\square$

**Theorem 2.** Consider the position control problem of the QUAV (11d)-(11f) under disturbances with Assumption 3. Then the AFONFTSMC approach in (24) and their adaptation laws (25)-(27), the tracking errors of outer-loop converge to zero in the finite times.

*Proof.* To prove the theorem 2, first, consider the Lyapunov function as

$$V^p = \frac{1}{2}(\mathbf{S}_x^p + \mathbf{S}_y^p + \mathbf{S}_z^p) + \sum_{i=1}^2 \left\{ \frac{\tilde{b}_{i7}^2}{2\eta_{xi}} + \frac{\tilde{b}_{i9}^2}{2\eta_{yi}} + \frac{\tilde{b}_{i11}^2}{2\eta_{zi}} \right\} \quad (35)$$

Next, after a simple calculus, the time-derivative of  $V^p$  satisfies the following inequality.

$$\begin{aligned} \dot{V}^p &\leq -(\hbar_{x1} + \mu) |\mathbf{S}_x^p| - \hbar_{x2} \mathbf{S}_x^{p2} - (\hbar_{y1} + \mu) |\mathbf{S}_y^p| \\ &\quad - \hbar_{y2} \mathbf{S}_y^{p2} - (\hbar_{z1} + \mu) |\mathbf{S}_z^p| - \hbar_{z2} \mathbf{S}_z^{p2} \end{aligned} \quad (36)$$

The control parameters should be selected by the positive gains; then  $\dot{V}^p$  is negative.  $\square$

### C. Rotational subsystem

In this subsection, the proposed controller will be applied for rotational trajectory-tracking control. The aim of this part is to generate the yawing, pitching, and rolling signal torques, which stabilize the QUAV system in the presence of random disturbances/uncertainties. The FONFT sliding manifolds for the attitude subsystem are chosen as follows:

$$\mathbf{S}_\phi^\varphi = \mathbf{e}_\phi^2 + D^{\gamma_{\phi1}-1} c_{\phi1} \mathbf{e}_\phi^{1p_\phi/q_\phi} + I^{\gamma_{\phi2}} c_{\phi2} \mathbf{e}_\phi^{1\varphi_\phi} sgn(\mathbf{e}_\phi^1) \quad (37)$$

$$\mathbf{S}_\theta^\varphi = \mathbf{e}_\theta^2 + D^{\gamma_{\theta1}-1} c_{\theta1} \mathbf{e}_\theta^{1p_\theta/q_\theta} + I^{\gamma_{\theta2}} c_{\theta2} \mathbf{e}_\theta^{1\varphi_\theta} sgn(\mathbf{e}_\theta^1) \quad (38)$$

$$\mathbf{S}_\psi^\varphi = \mathbf{e}_\psi^2 + D^{\gamma_{\psi1}-1} c_{\psi1} \mathbf{e}_\psi^{1p_\psi/q_\psi} + I^{\gamma_{\psi2}} c_{\psi2} \mathbf{e}_\psi^{1\varphi_\psi} sgn(\mathbf{e}_\psi^1) \quad (39)$$

where  $c_{j1}$ ,  $c_{j2}$ , and  $\varphi_j$  for  $j = \phi, \theta, \psi$  are positive parameters. The parameters  $p_j$  and  $q_j$  satisfied that  $1 < p_j/q_j < 2$ . The fractional operators  $\gamma_{j1}$  and  $\gamma_{j2}$  are  $0 < \gamma_{j1}, \gamma_{j2} < 1$ . The  $\mathbf{e}_j^1$  is the tracking error and its derivative  $\dot{\mathbf{e}}_j^1 = \mathbf{e}_j^2 |_{j=\phi,\theta,\psi}$  defined as:

$$\mathbf{e}_\phi^1 = \phi - \phi^r, \quad \mathbf{e}_\theta^1 = \theta - \theta^r, \quad \mathbf{e}_\psi^1 = \psi - \psi^r \quad (40)$$

$$\mathbf{e}_\phi^2 = \dot{\phi} - \dot{\phi}^r, \quad \mathbf{e}_\theta^2 = \dot{\theta} - \dot{\theta}^r, \quad \mathbf{e}_\psi^2 = \dot{\psi} - \dot{\psi}^r \quad (41)$$

Similar design procedure to that presented in the previous part can be conducted to design FOANFTSMC laws for path following control of roll, pitch, and yaw angles.

The corresponding signal inputs for the rotational subsystem are developed as follows:

$$\begin{aligned} \tau_x &= \frac{1}{a_{\Phi_1}} [-\{a_{\phi_1}\dot{\phi}\dot{\psi} - a_{\phi_2}\dot{\phi}\dot{\varphi} - a_{\phi_3}\dot{\phi}^2\} + \ddot{\phi}^r - D^{\gamma_{\phi1}} c_{x1} \mathbf{e}_\phi^{1p_\phi/q_\phi} \\ &\quad - I^{\gamma_{\phi2}} c_{\phi2} \varphi_\phi |\mathbf{e}_\phi^1|^{\varphi_\phi-1} \mathbf{e}_\phi^2 - \hbar_{\phi1} sgn(\mathbf{S}_\phi^\varphi) - \hbar_{\phi2} \mathbf{S}_\phi^\varphi \\ &\quad + (\hat{b}_{01} + \hat{b}_{11} \mathbf{e}_\phi^1 + \hat{b}_{21} \mathbf{e}_\phi^2 + \mu) sgn(\mathbf{S}_\phi^\varphi)] \end{aligned} \quad (42)$$

$$\begin{aligned} \tau_y &= \frac{1}{a_{\Theta_1}} [-\{a_{\theta_1}\dot{\phi}\dot{\psi} + a_{\theta_2}\dot{\phi}\dot{\varphi} - a_{\theta_3}\dot{\phi}^2\} + \ddot{\theta}^r - D^{\gamma_{\theta1}} c_{\theta1} \mathbf{e}_\theta^{1p_\theta/q_\theta} \\ &\quad - I^{\gamma_{\theta2}} c_{\theta2} \varphi_\theta |\mathbf{e}_\theta^1|^{\varphi_\theta-1} \mathbf{e}_\theta^2 - \hbar_{\theta1} sgn(\mathbf{S}_\theta^\varphi) - \hbar_{\theta2} \mathbf{S}_\theta^\varphi \\ &\quad - (\hat{b}_{03} + \hat{b}_{13} \mathbf{e}_\theta^1 + \hat{b}_{23} \mathbf{e}_\theta^2 + \mu) sgn(\mathbf{S}_\theta^\varphi)] \end{aligned} \quad (43)$$

$$\begin{aligned} \tau_z &= \frac{1}{a_{\Psi_1}} [-\{a_{\psi_1}\dot{\phi}\dot{\psi} - a_{\psi_2}\dot{\phi}\dot{\varphi} - a_{\psi_3}\dot{\phi}^2\} + \ddot{\psi}^r - D^{\gamma_{\psi1}} c_{\psi1} \mathbf{e}_\psi^{1p_\psi/q_\psi} \\ &\quad - I^{\gamma_{\psi2}} c_{\psi2} \varphi_\psi |\mathbf{e}_\psi^1|^{\varphi_\psi-1} \mathbf{e}_\psi^2 - \hbar_{\psi1} sgn(\mathbf{S}_\psi^\varphi) - \hbar_{\psi2} \mathbf{S}_\psi^\varphi \\ &\quad - (\hat{b}_{05} + \hat{b}_{15} \mathbf{e}_\psi^1 + \hat{b}_{25} \mathbf{e}_\psi^2 + \mu) sgn(\mathbf{S}_\psi^\varphi)] \end{aligned} \quad (44)$$

with  $\hbar_{j1}$  and  $\hbar_{j2}$  are the control parameters.  $\hat{b}_{0k}$ ,  $\hat{b}_{1k}$ , and  $\hat{b}_{2k}$  for  $k = 1, 3, 5$  are updated by the adaptive laws formulated as:

$$\dot{\hat{b}}_{01} = \eta_{\phi1} |\mathbf{S}_\phi^\varphi|, \quad \dot{\hat{b}}_{11} = \eta_{\phi1} \mathbf{e}_\phi^1 |\mathbf{S}_\phi^\varphi|, \quad \dot{\hat{b}}_{21} = \eta_{\phi2} \mathbf{e}_\phi^2 |\mathbf{S}_\phi^\varphi| \quad (45)$$

$$\dot{\hat{b}}_{03} = \eta_{\theta1} |\mathbf{S}_\theta^\varphi|, \quad \dot{\hat{b}}_{13} = \eta_{\theta1} \mathbf{e}_\theta^1 |\mathbf{S}_\theta^\varphi|, \quad \dot{\hat{b}}_{23} = \eta_{\theta2} \mathbf{e}_\theta^2 |\mathbf{S}_\theta^\varphi| \quad (46)$$

$$\dot{\hat{b}}_{05} = \eta_{\psi1} |\mathbf{S}_\psi^\varphi|, \quad \dot{\hat{b}}_{15} = \eta_{\psi1} \mathbf{e}_\psi^1 |\mathbf{S}_\psi^\varphi|, \quad \dot{\hat{b}}_{25} = \eta_{\psi2} \mathbf{e}_\psi^2 |\mathbf{S}_\psi^\varphi| \quad (47)$$

where  $\eta_{j0}$ ,  $\eta_{j1}$ , and  $\eta_{j2}$  for  $j = \phi, \theta, \psi$  to be designed.

**Theorem 3.** Consider the rotational subsystem described in (11a)-(11c), if the control signals  $\tau_x$ ,  $\tau_y$  and  $\tau_z$  are developed as in (42)-(44) with the adaptation laws in (45)-(47), which has existing uncertainties/disturbances, with the proposed FONFTS surfaces presented in (37)-(39), then the closed-loop attitude subsystem will converge in a finite time for every initial condition.

*Proof.* In order to prove the stability of the attitude subsystem, the Lyapunov function can be chosen as

$$V^{\eta\varphi} = \frac{1}{2}(\mathbf{S}_\phi^{\varphi2} + \mathbf{S}_\theta^{\varphi2} + \mathbf{S}_\psi^{\varphi2}) + \sum_{i=1}^2 \left\{ \frac{\tilde{b}_{i1}^2}{2\eta_{\phi i}} + \frac{\tilde{b}_{i3}^2}{2\eta_{\theta i}} + \frac{\tilde{b}_{i5}^2}{2\eta_{\psi i}} \right\} \quad (48)$$

The same calculus presented in the previous section for the translational subsystem can be used to obtain the differential inequality of the  $V^{\eta\varphi}$ . Then, The time-derivative of  $V^{\eta\varphi}$  can be given by the following differential-inequality.

$$\begin{aligned} \dot{V}^{\eta\varphi} &\leq -(\hbar_{\phi1} + \mu) |\mathbf{S}_\phi^\varphi| - \hbar_{x2} \mathbf{S}_\phi^{p2} - (\hbar_{\theta1} + \mu) |\mathbf{S}_\theta^\varphi| \\ &\quad - \hbar_{y2} \mathbf{S}_y^{p2} - (\hbar_{z1} + \mu) |\mathbf{S}_z^\varphi| - \hbar_{z2} \mathbf{S}_z^{p2} \end{aligned} \quad (49)$$

The control parameters should be selected by the positive gains; then  $\dot{V}^{\eta\varphi}$  is negative. Then, the rotational stability is ensured by (42)-(44) in the presence of external disturbances.  $\square$

**Theorem 4.** The ultimate control signals (28), (42), (43), and (44) applied to the QUAV dynamics presented in (11a) to (11f) with the ultimate adaptive laws designed in (25)-(27) and (45)-(47) guarantee the overall closed-loop QUAV system stability.

*Proof.* The Lyapunov function for the overall QUAV system is defined as:

$$\mathcal{V}_{QAV} = V^{\eta\varphi} + V^p \quad (50)$$

The time-derivative of  $\mathcal{V}_{QAV}$  is,

$$\dot{\mathcal{V}}_{QAV} = \dot{V}^{\eta\varphi} + \dot{V}^p \quad (51)$$

Using the equations (36) and (49), we have,

$$\begin{aligned} \dot{\mathcal{V}}_{QAV} &\leq -(\hbar_{x1} + \mu) |\mathbf{S}_x^p| - \hbar_{x2} \mathbf{S}_x^{p2} - (\hbar_{y1} + \mu) |\mathbf{S}_y^p| \\ &\quad - \hbar_{y2} \mathbf{S}_y^{p2} - (\hbar_{z1} + \mu) |\mathbf{S}_z^p| - \hbar_{z2} \mathbf{S}_z^{p2} \\ &\quad - (\hbar_{\phi1} + \mu) |\mathbf{S}_\phi^\varphi| - \hbar_{x2} \mathbf{S}_\phi^{p2} - (\hbar_{\theta1} + \mu) |\mathbf{S}_\theta^\varphi| \\ &\quad - \hbar_{y2} \mathbf{S}_y^{p2} - (\hbar_{\psi1} + \mu) |\mathbf{S}_\psi^\varphi| - \hbar_{z2} \mathbf{S}_z^{p2} \\ &\leq 0 \end{aligned} \quad (52)$$

From the above analysis, the global stability of the overall QUAV system is proved.  $\square$

**Remark 2.** As seen, the FO control method proposed in this work achieves fast position and attitude regulation with

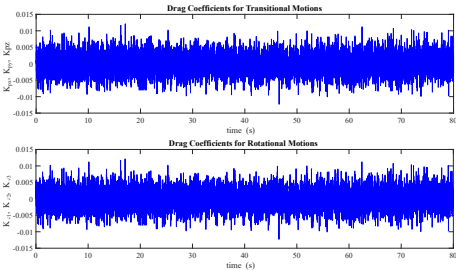


Fig. 3: The imitated drag coefficients.

parameters high accuracy in the presence of random uncertainties/disturbances. The computational cost of the FONFTSMC technique is similar to most recent developed works in Refs. [18], [19], [21], [22], [26]. Thus, the complexity of the proposed method is similar to them. Compared with other existing nonlinear controllers, the FONFTSMC has many characteristics such as simplicity, fast finite-time speed of convergence, chatter-free control inputs, low hardware requirement, and nonsingularity.

## V. SIMULATION RESULTS

In the following section, simulation studies under several scenarios are given to validate the superiority of the AFONFTSMC scheme proposed in this work. Besides, comprehensive comparisons on the feedback linear (FL) [37], backstepping sliding mode control (BSMC) [9], [10], fractional-order BSMC [17], and nonsingular fast terminal sliding mode control methods [26] are conducted. Consider the nominal parameters of the QUAV used in following simulations as [45]:  $barm = 0.74kg$ ,  $\bar{I} = diag[0.4, 0.4, 0.84]10^{-2}kg.m^2$ ,  $\bar{K}_p = diag[1, 1, 1]10^{-2}Nsm^{-1}$ ,  $\bar{K}_\varphi = diag[1.2, 1.2, 1.2]10^{-2}Nsrad^{-1}$ ,  $\rho_b = 310^{-3}Ns^2$ ,  $\rho_c = 3.2410^{-2}Nm s^2$  and  $d = 0.21m$ . where  $\bar{I}$ ,  $\bar{m}$ ,  $\bar{K}_p$ , and  $\bar{K}_\varphi$  denote the nominal values respectively of  $I$ ,  $m$ ,  $K_p$  and  $K_\varphi$ . The initial conditions  $[0.05, 0.01, 0]m$  and  $[0.01, 0.01, 0.1]rad$  have been considered in all scenarios.

**Remark 3.** In order to reach the trajectory-tracking satisfied performance of the quadrotor system in the presence of random disturbances/uncertainties, the designed parameters of the controllers should be tuned. Using MATLAB optimization toolbox (see Ref. [46]) we selected the best values of those parameters.

For all proposed cases, the position and attitude control parameters are considered as  $c_{x1} = c_{y1} = 0.1797$ ,  $c_{x2} = c_{y2} = 0.1769$ ,  $c_{z1} = 4.4265$ ,  $c_{z2} = 3.7049$ ,  $c_{\phi 1} = c_{\theta 1} = c_{\psi 1} = 35.5118$ ,  $c_{\phi 2} = c_{\theta 2} = c_{\psi 2} = 3.9926$ ,  $\hbar_{x1} = \hbar_{y1} = 2.6044$ ,  $\hbar_{z1} = 16.1251$ ,  $\hbar_{\phi 1} = \hbar_{\theta 1} = \hbar_{\psi 1} = 156.4373$ ,  $\hbar_{x2} = \hbar_{y2} = 0.2204$ ,  $\hbar_{z2} = 0.8876$ ,  $\hbar_{\phi 2} = \hbar_{\theta 2} = \hbar_{\psi 2} = 5.8670$ ,  $\varphi_i = \varphi_j = 3$ ,  $p_i = p_j = 11$ ,  $q_i = q_j = 10$ ,  $\eta_{i0} = \eta_{j0} = 0.01$ ,  $\eta_{i1} = \eta_{j1} = 0.01$ ,  $\eta_{i2} = \eta_{j2} = 0.01$ ,  $\gamma_{i1} = \gamma_{j1} = 0.99$ , and  $\gamma_{i2} = \gamma_{j2} = 0.01$ .

In order to fully validate the performance and robustness of the AFONFTSMC approach, three operational scenarios are demonstrated, which are explained as follows. In Scenario 1, the random variation of the rotational and translational drag coefficients is considered. This effect is presented in Fig. 3. Also, to show the capability of the proposed controller,

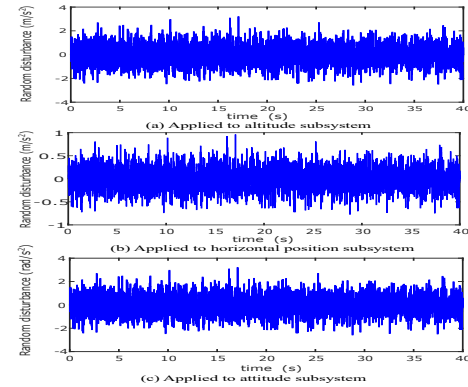


Fig. 4: Gaussian random disturbances.

external disturbances are introduced in the simulation. In Scenario 2, in addition to the effect of the drag coefficients considered in Scenario 1, random Gaussian disturbances affected the QUAV dynamics are considered, which are displayed in Fig. 4. In Scenario 3, the 30 randomly uncertainty of the mass and moment of inertia are considered, which can be given as:  $I_{11} = \bar{I}_{11}(1 + Random[0, 30\%])$ ;  $I_{22} = \bar{I}_{22}(1 + Random[0, 30\%])$ ;  $I_{33} = \bar{I}_{33}(1 + Random[0, 30\%])$ ,  $m = \bar{m}(1 + Random[0, 30\%])$ ; to further demonstrate the superiority of the proposed AFONFTSMC, external disturbances are also taking into account.

**Remark 4.** The CRONE method was considered in the numerical simulations to approximate the fractional dynamics of the proposed controller. The fractional term is replaced by a transfer function of order 10 with a frequency range from 0.01 to 100 rad = s.

### A. With Drag Coefficients Uncertainties and Stochastic Disturbances

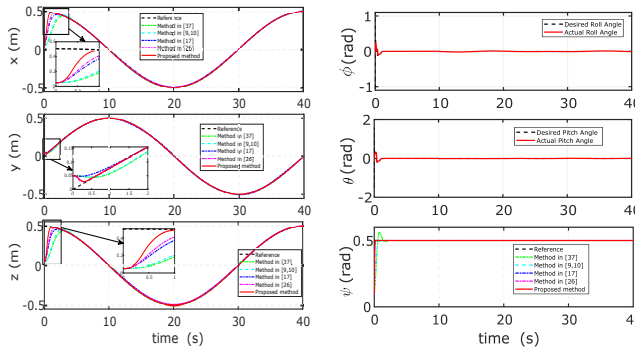
The external disturbances considered in this scenario are given by:

$$\begin{aligned} d_{px}(t) &= -(0.08 \sin(0.11t - 3.0403) + 0.04 \sin(0.5t - 13.5) \\ &\quad + 0.008 \sin(1.6t - 15\pi) + 0.006 \sin(0.3t - 8.6)) \\ &\quad m/s^2 \quad t \in [10, 30] \\ &= 0 \quad m/s^2 \quad \text{otherwise} \\ d_{py}(t) &= 0.05 \sin(0.4t) + 0.05 \cos(0.7t) \quad m/s^2 \quad t \in [10, 50] \\ &= 0 \quad m/s^2 \quad \text{otherwise} \\ d_{pz}(t) &= 0.05 \cos(0.7t) + 0.07 \sin(0.3) \quad m/s^2 \quad t \in [0, 80] \\ d_{\varphi 1} &= 0.5 \cos(0.4t) + 1 \quad rad/s^2 \quad t \in [0, 80] \\ d_{\varphi 2} &= 0.5 \sin(0.5t) + 1 \quad rad/s^2 \quad t \in [0, 80] \\ d_{\varphi 3} &= 0.05 \sin(0.7 * t) + 0.1 \quad rad/s^2 \quad t \in [0, 80] \end{aligned} \quad (53)$$

In this part, the QUAV is ordered to follow the reference yaw angle and position as follows:

$$x^r = 0.5 \cos(\frac{\pi}{20})m, \quad y^r = 0.5 \sin(\frac{\pi}{20})m \quad (54)$$

$$z^r = 2 - 2 \cos(\frac{\pi}{2})m, \quad \psi^r = 0.5rad \quad (55)$$



(a) Position tracking.

(b) Attitude tracking.

Fig. 5: Path following performance in Scenario 1.

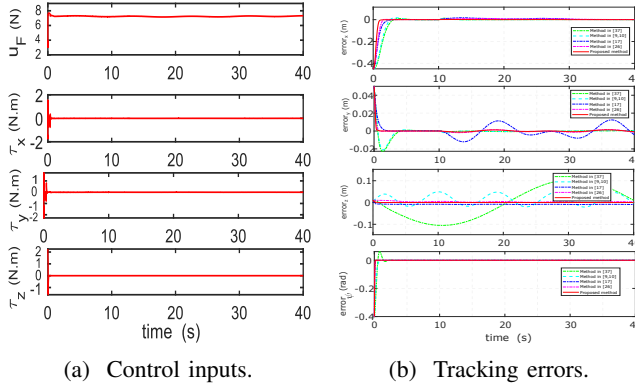


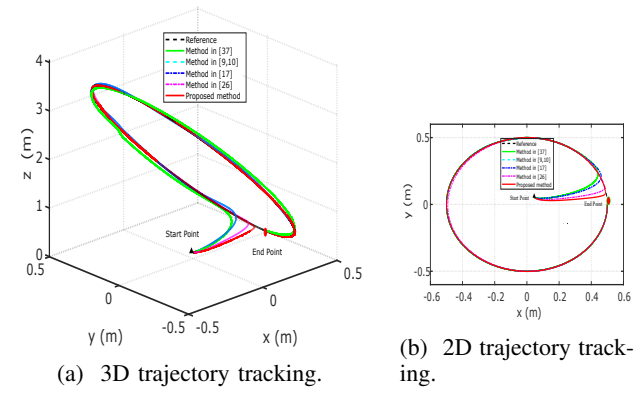
Fig. 6: Control inputs & tracking errors in Scenario 1.

The simulation results obtained in this scenario by several control methods and the proposed FONFTSMC method are plotted in Figs. 5a-8b. The tracking control performance of position/attitude is shown in Figs. 5a and 5b. In the presence of drag coefficient influences and significant disturbances, the AFONFTSMC can be precisely tracked the desired QUAV states. Corresponding signal inputs are depicted in Fig. 6a. These results confirm the efficiency of the proposed controller. From Fig. 6b, we can observe that both position and velocity tracking errors converge to zero in finite time. The results of the path following in 3-D and 2-D spaces are respectively shown in Fig. 7a and Fig. 7b. It can be observed that all control approaches can successfully perform the trajectories tracking in the presence of uncertainties drag coefficients/perturbations. The attitude and position parameter adaptations are shown in Fig. 8a and Fig. 8b respectively.

Therefore, during the first period of flight, the AFONFTSMC has better performances in terms of overshoot, settling/rising time, and steady-state error than other compared techniques. Also, the proposed method can obtain the better robustness performances relative to external disturbances and uncertainties.

#### B. With Drag Coefficients Uncertainties and Random disturbances

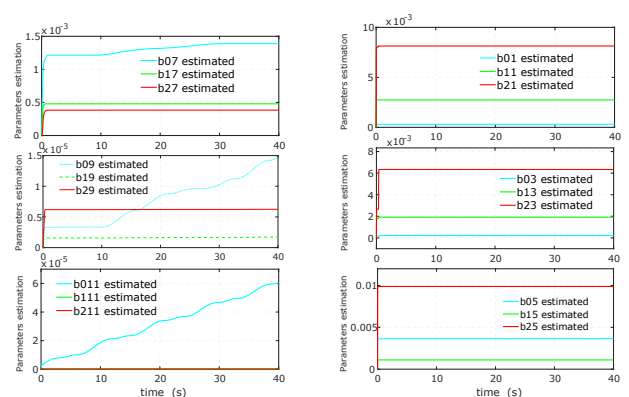
In this case, the negative effect of random disturbances affecting the dynamics of the QUAV is taken into account to



(a) 3D trajectory tracking.

(b) 2D trajectory tracking.

Fig. 7: Path following performance in Scenario 1.



(a) Parameters position.

(b) Parameters attitude.

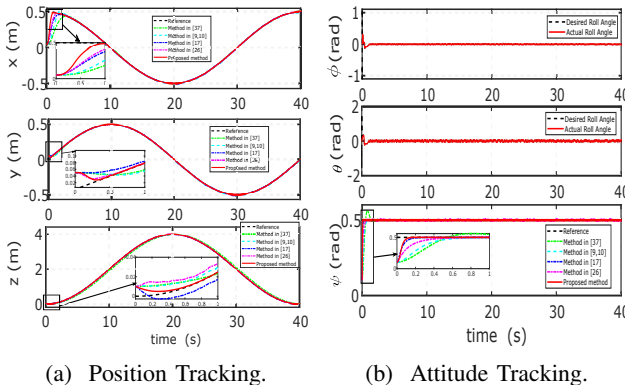
Fig. 8: Parameters estimation in Scenario 1.

demonstrate the effectiveness of the control strategy proposed in this work. The tracking performance of the QUAV via the five techniques is presented in Fig. 9a and Fig. 9b shows the responses of the attitude and position of all controllers with extra random disturbances applied. It is shown that good performances are achieved via the proposed method. This is confirmed by the results of the tracking errors demonstrated in Fig. 10b. Moreover, Fig. 10a illustrates the trajectories of thrust  $u_F$ , roll  $\tau_x$ , pith  $\tau_y$  and yaw  $\tau_z$  moments applied to the QUAV. The 3-D and 2-D trajectories of the proposed controller are presented in Figs. 11a and 11b. It can be found that the QUAV's path following can rapidly track the desired ones even in the presence of random disturbances. The response of parameter estimations for the attitude and position are shown respectively in Fig. 12a and Fig. 12b.

Hence, the comparative simulations of AFONFTSMC method against other approaches are improved and better in terms of convergence speed, trajectory tracking, and rejection of the random disturbances.

#### C. With Random Uncertainties (Random uncertainty 30% added in mass and rotary inertia) and External Disturbances

In this scenario, the Random uncertainty 30% is added in the nominal parameters of the mass and rotary inertia to further verify the suggested control strategy. Also, the external



(a) Position Tracking. (b) Attitude Tracking.

Fig. 9: Path following performance in Scenario 2.

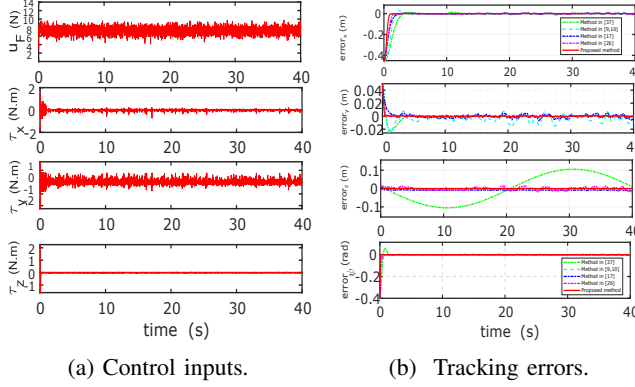


Fig. 10: Control inputs & tracking errors in Scenario 2.

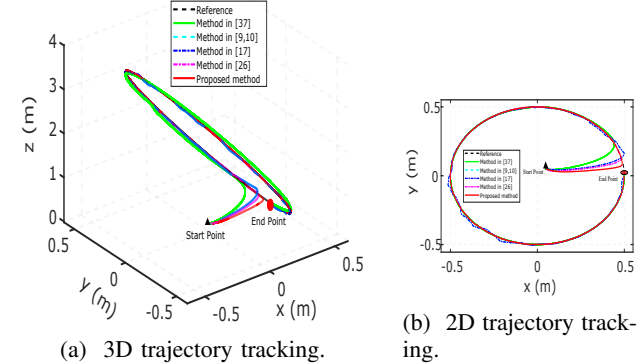
disturbances are considered, which are formulated as:

$$\begin{aligned} d_{px}(t) &= 0.3 \sin(2t) + 0.1 \sin(3t) m/s^2 \\ d_{py}(t) &= 0.2 \cos(2t) + 0.2 \sin(2t) m/s^2 \\ d_{pz}(t) &= 0.5 \cos(2t) + 0.7 \sin(3t) m/s^2 \\ d_{\varphi 1} &= 0.9 \cos(0.4t) + 2.2 \sin(2t) rad/s^2 \\ d_{\varphi 2} &= 0.8 \sin(t) + 1.4 \cos(2t) rad/s^2 \\ d_{\varphi 3} &= 1.3 \sin(5t) + 1.5 \cos(3t) rad/s^2 \end{aligned} \quad (56)$$

The reference trajectory is defined as follows:

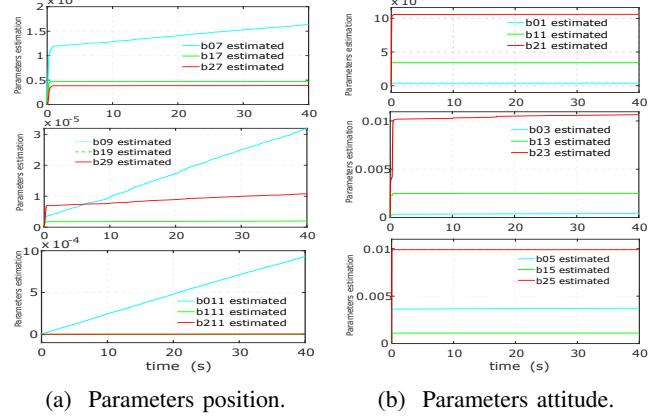
$$\begin{aligned} x^r &= \begin{cases} 0 & m \ t \in [0, 7] \\ 10[1 - \cos(\frac{2\pi(t-7)}{23})] & m \ t \in [7, 50] \end{cases} \\ y^r &= \begin{cases} 0 & m \ t \in [0, 7] \\ 5 \sin(\frac{4\pi(t-7)}{23}) & m \ t \in [7, 50] \end{cases} \\ z^r &= 7(1 - \exp(-0.3t)) \ m \\ \psi^r &= 0.5 \ rad \end{aligned} \quad (57)$$

Simulation results on the entire control techniques used for the comparison and the proposed control scheme are shown in Figs. 13a-16b, from which we can observe that position and attitude tracking, signal control inputs, tracking errors, path-following in 3-D and 2-D spaces, and estimates on parameters can be obtained with high accuracy. Under the aforementioned perturbations affected the QUAV dynamics, it can be figured out the random uncertainties have major impacts on other methods. However, comparing Figs. 13a and 14b, we can see that the proposed AFONFTSMC scheme can obtain more



(a) 3D trajectory tracking. (b) 2D trajectory tracking.

Fig. 11: Path following performance in Scenario 2.



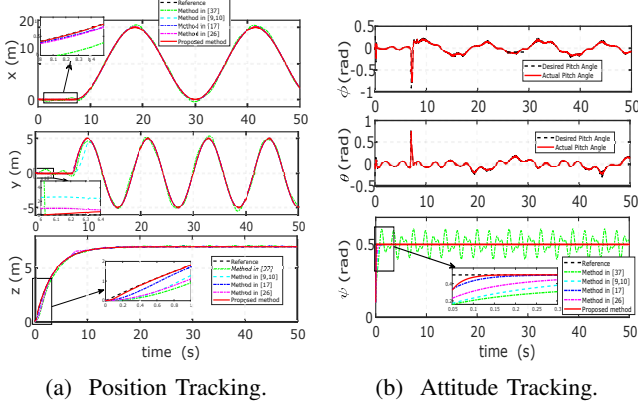
(a) Parameters position. (b) Parameters attitude.

Fig. 12: Parameters estimation in Scenario 2.

accurate trajectory tracking, stronger random uncertainty and disturbances rejection, simultaneously. The results in 3D and 2-D spaces presented in Figs. 15b and 15b further validated the properties of the proposed approach.

In summary, the AFONFTSMC method proposed in this work can achieve an exact trajectory tracking in the presence of perturbations including random uncertainties and/or disturbances.

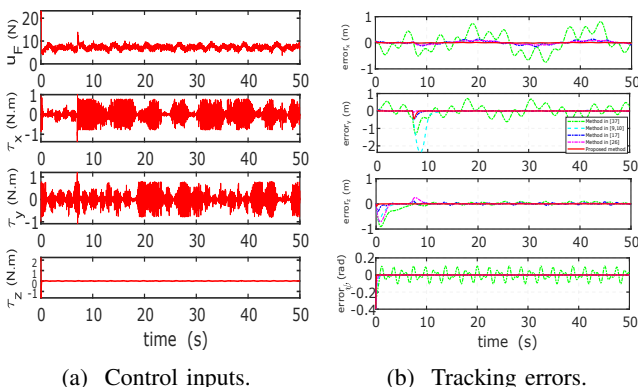
**Remark 5.** This note goes at describing the procedure for experimental validation of the proposed scheme [47], [48]. In this context to build the QUAV test bench and validate the proposed scenarios, a list of the pieces of equipment has been compiled. Fig. 17 displays the hardware configuration of the QUAV experimental platform. The platform uses the X450 quadrotor with one ground control station (GCS), DSP TMS320F28379D, Inertial Measurement Unit (IMU) that includes 3-axis magnetometer, 3-axis gyroscope, and 3-axis accelerometer, the global positioning system (GPS) module measures the velocity and position in the horizontal plane. While the barometric sensor measure the altitude. To ensure communication between QUAV and the ground station, two Zigbee wireless modules were used. The disturbance is caused by wind generated by a fan. A micro SD card saves the flight parameters onboard.



(a) Position Tracking.

(b) Attitude Tracking.

Fig. 13: Path following performance in Scenario 3.



(a) Control inputs.

(b) Tracking errors.

Fig. 14: Control inputs & tracking errors in Scenario 3.

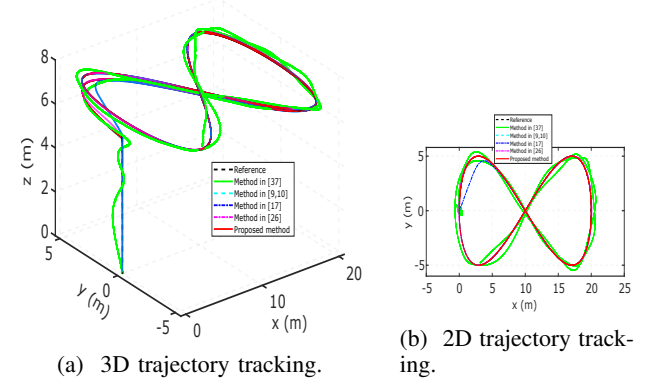
## VI. CONCLUSIONS

In this paper, an adaptive fractional-order nonsingular fast terminal sliding mode control (AFONFTSMC) scheme is proposed for the QUAV copter against random/multiple parametric uncertainties, and external disturbances while improving the path following performance. The influence of drag coefficients, mass/inertia-moment variations, and random time-varying disturbances are compensated by using the proposed control approach based on adaptive laws. The FONFTESMC adopted for the QUAV has provided rapid FT convergence, improved the performance of trajectory tracking, and avoided the chattering/singularity problems. The robustness of the FO control approach proposed in this work is discussed by three different scenarios with regard to random uncertainties/disturbances. Finally, three simulation results conducted in the different cases have shown the AFONFTSMC superiority recently published controllers in the term of fast finite-time convergence, smaller tracking errors, and rejection of the uncertainties/disturbances.

The proposed control scheme (FONFTESMC) will be validated by experiment in future work.

## REFERENCES

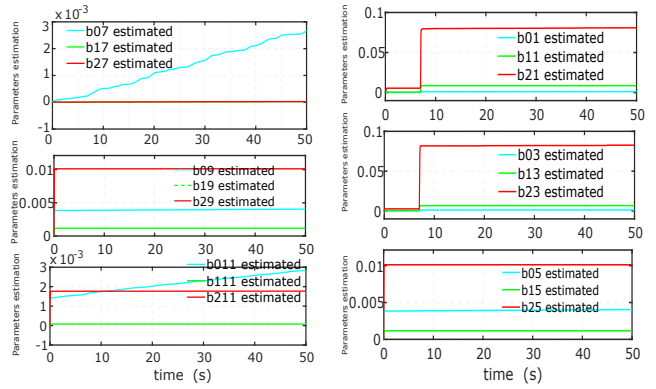
- [1] Z. Zuo and P. Ru, Augmented script L1 adaptive tracking control of quad-rotor unmanned aircrafts, *IEEE Trans. Aerosp. Electron. Syst.*, vol. 50, no. 4, pp. 30903101, 2014.



(a) 3D trajectory tracking.

(b) 2D trajectory tracking.

Fig. 15: Path following performance in Scenario 3.



(a) Parameters position.

(b) Parameters attitude.

Fig. 16: Parameters estimation in Scenario 3.

- [2] L. Qian and H. H. T. Liu, Path-Following Control of A Quadrotor UAV with A Cable-Suspended Payload under Wind Disturbances, *IEEE Trans. Ind. Electron.*, vol. 67, no. 3, pp. 20212029, 2020.
- [3] P. Chen, Z. Xie, Y. Fang, Z. Chen, S. Mumtaz and J. J. P. C. Rodrigues, "Physical-Layer Network Coding: An Efficient Technique for Wireless Communications," in *IEEE Network*, vol. 34, no. 2, pp. 270-276, March/April 2020.
- [4] H. Liu, W. Zhao, Z. Zuo, and Y. Zhong, Robust Control for Quadrotors with Multiple Time-Varying Uncertainties and Delays, *IEEE Trans. Ind. Electron.*, vol. 64, no. 2, pp. 13031312, 2017.
- [5] K. Zhao, J. Zhang, D. Ma and Y. Xia, Composite Disturbance Rejection Attitude Control for Quadrotor with Unknown Disturbance, *IEEE Trans. Ind. Electron.*, vol. 67, no. 8, pp. 68946903, 2020.
- [6] W. Lei, C. Li, and M. Z. Q. Chen, Robust Adaptive Tracking Control for Quadrotors by Combining PI and Self-Tuning Regulator, *IEEE Trans. Control Syst. Technol.*, vol. 27, no. 6, pp. 26632671, 2019.
- [7] G. Yu, D. Cabecinhas, R. Cunha, and C. Silvestre, Nonlinear Backstepping Control of a Quadrotor-Slung Load System, *IEEE/ASME Trans. Mechatronics*, vol. 24, no. 5, pp. 23042315, 2019.
- [8] N. Wang, S. F. Su, M. Han, and W. H. Chen, Backpropagating

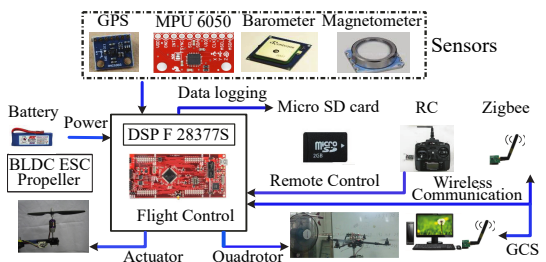


Fig. 17: The quadrotor's hardware structure.

- Constraints-Based Trajectory Tracking Control of a Quadrotor With Constrained Actuator Dynamics and Complex Unknowns, *IEEE Trans. Syst. Man, Cybern. Syst.*, pp. 116, 2018.
- [9] F. Chen, R. Jiang, K. Zhang, B. Jiang, and G. Tao, Robust Backstepping Sliding-Mode Control and Observer-Based Fault Estimation for a Quadrotor UAV, *IEEE Trans. Ind. Electron.*, vol. 63, no. 8, pp. 50445056, 2016.
- [10] M. A. M. Basri, Design and application of an adaptive backstepping sliding mode controller for a six-DOF quadrotor aerial robot, *Robotica*, vol. 36, no. 11, pp. 17011727, Aug. 2018.
- [11] X. Liang, Y. Fang, N. Sun, and H. Lin, A novel energy-coupling-based hierarchical control approach for unmanned quadrotor transportation systems, *IEEE/ASME Trans. Mechatronics*, vol. 24, no. 1, pp. 248-259, 2019.
- [12] A. Noormohammadi-Asl, O. Esrafilian, M. Ahangar Arzati, and H. D. Taghirad, System identification and H<sub>8</sub>-based control of quadrotor attitude, *Mech. Syst. Signal Process.*, vol. 135, p. 106358, 2020.
- [13] A. Chamseddine, Y. Zhang, C. A. Rabbath, C. Join, and D. Theilliol, Flatness-Based Trajectory Planning/Replanning for a Quadrotor Unmanned Aerial Vehicle, *IEEE Transactions on Aerospace and Electronic Systems*, vol. 48, no. 4, pp. 28322848, Oct. 2012.
- [14] X. Wang and B. Shirinzadeh, Nonlinear multiple integrator and application to aircraft navigation, *IEEE Trans. Aerosp. Electron. Syst.*, vol. 50, no. 1, pp. 607622, 2014.
- [15] H. Wang, X. Ye, Y. Tian, G. Zheng, and N. Christov, Model-freebased terminal SMC of quadrotor attitude and position, *IEEE Transactions on Aerospace and Electronic Systems*, vol. 52, no. 5, pp. 25192528, Oct. 2016.
- [16] M. Labbadi and M. Cherkaoui, Robust adaptive backstepping fast terminal sliding mode controller for uncertain quadrotor UAV, *Aerospace Science and Technology*, vol. 93, p. 105306, 2019.
- [17] X. Shi, Y. Cheng, C. Yin, S. Dadras, and X. Huang, Design of Fractional-Order Backstepping Sliding Mode Control for Quadrotor UAV, *Asian Journal of Control*, vol. 21, no. 1, pp. 156171, Nov. 2018.
- [18] S. Y. Chen, H. H. Chiang, T. S. Liu, and C. H. Chang, Precision Motion Control of Permanent Magnet Linear Synchronous Motors Using Adaptive Fuzzy Fractional-Order Sliding-Mode Control, *IEEE/ASME Trans. Mechatronics*, vol. 24, no. 2, pp. 741752, 2019.
- [19] D. Nojavan-zadeh and M. Badamchizadeh, Adaptive fractional-order non-singular fast terminal sliding mode control for robot manipulators, *IET Control Theory Appl.*, vol. 10, no. 13, pp. 15651572, 2016.
- [20] S. Xu, G. Sun, Z. Ma, and X. Li, Fractional-Order Fuzzy Sliding Mode Control for the Deployment of Tethered Satellite System under Input Saturation, *IEEE Trans. Aerosp. Electron. Syst.*, vol. 55, no. 2, pp. 747756, 2019.
- [21] S. Xu, G. Sun, Z. Ma, and X. Li, Fractional-Order Fuzzy Sliding Mode Control for the Deployment of Tethered Satellite System under Input Saturation, *IEEE Trans. Aerosp. Electron. Syst.*, vol. 55, no. 2, pp. 747756, 2019.
- [22] Y. Wang, J. Chen, F. Yan, K. Zhu, and B. Chen, Adaptive super-twisting fractional-order nonsingular terminal sliding mode control of cable-driven manipulators, *ISA Trans.*, vol. 86, pp. 163180, 2019.
- [23] H. Rios, R. Falcon, O. A. Gonzalez, and A. Dzul, Continuous Sliding-Mode Control Strategies for Quadrotor Robust Tracking: Real-Time Application, *IEEE Trans. Ind. Electron.*, vol. 66, no. 2, pp. 12641272, 2019.
- [24] V. P. Tran, F. Santoso, M. A. Garratt, and I. R. Petersen, Adaptive Second-Order Strictly Negative Imaginary Controllers Based on the Interval Type-2 Fuzzy Self-Tuning Systems for a Hovering Quadrotor with Uncertainties, *IEEE/ASME Trans. Mechatronics*, vol. 25, no. 1, pp. 1120, 2020.
- [25] C. Izaguirre-Espinosa, A. J. Munoz-Vazquez, A. Sanchez-Orta, V. Parra-Vega, and I. Fantoni, Fractional-Order Control for Robust Position/Yaw Tracking of Quadrotors With Experiments, *IEEE Transactions on Control Systems Technology*, vol. 27, no. 4, pp. 16451650, Jul. 2019.
- [26] M. Labbadi and M. Cherkaoui, Robust adaptive nonsingular fast terminal sliding-mode tracking control for an uncertain quadrotor UAV subjected to disturbances, *ISA Trans.*, vol. 99, pp. 290304, 2020.
- [27] C. Izaguirre-Espinosa, A. J. Muoz-Vzquez, A. Snchez-Orta, V. Parra-Vega, and P. Castillo, Attitude control of quadrotors based on fractional sliding modes: Theory and experiments, *IET Control Theory Appl.*, vol. 10, no. 7, pp. 825832, 2016.
- [28] F. Oliva-Palomo, A. J. Munoz-Vazquez, A. Sanchez-Orta, V. Parra-Vega, C. Izaguirre-Espinosa, and P. Castillo, A Fractional Nonlinear PI-structure Control for Robust Attitude Tracking of Quadrotors, *IEEE Trans. Aerosp. Electron. Syst.*, vol. 9251, no. c, pp. 110, 2019.
- [29] W. Cai, J. She, M. Wu, and Y. Ohyama, Quadrotor waypoint-tracking control under exogenous disturbances based on equivalent-input-disturbance approach, *J. Franklin Inst.*, vol. 357, pp. 47094741, 2020.
- [30] Z. Xu, X. Nian, H. Wang, and Y. Chen, Robust guaranteed cost tracking control of quadrotor UAV with uncertainties, *ISA Trans.*, vol. 69, pp. 157165, 2017.
- [31] C. Mu and Y. Zhang, Learning-Based Robust Tracking Control of Quadrotor with Time-Varying and Coupling Uncertainties, *IEEE Trans. Neural Networks Learn. Syst.*, vol. 31, no. 1, pp. 259273, 2020.
- [32] Q. Xu, Z. Wang, and Z. Zhen, Information fusion estimation-based path following control of quadrotor UAVs subjected to Gaussian random disturbance, *ISA Trans.*, vol. 99, pp. 8494, 2020.
- [33] Q. Xu, Z. Wang, and Z. Zhen, Adaptive neural network finite time control for quadrotor UAV with unknown input saturation, *Nonlinear Dyn.*, vol. 98, no. 3, pp. 19731998, 2019.
- [34] Q. Chen, S. Xie, M. Sun, and X. He, Adaptive Nonsingular Fixed-Time Attitude Stabilization of Uncertain Spacecraft, *IEEE Trans. Aerosp. Electron. Syst.*, vol. 54, no. 6, pp. 29372950, 2018.
- [35] L. Zhao, J. Yu, and H. Yu, Adaptive Finite-Time Attitude Tracking Control for Spacecraft with Disturbances, *IEEE Trans. Aerosp. Electron. Syst.*, vol. 54, no. 3, pp. 12971305, 2018.
- [36] X. N. Shi, Y. A. Zhang, and D. Zhou, Almost-Global Finite-Time Trajectory Tracking Control for Quadrotors in the Exponential Coordinates, *IEEE Trans. Aerosp. Electron. Syst.*, vol. 53, no. 1, pp. 91100, 2017.
- [37] H. Voos, Nonlinear control of a quadrotor micro-UAV using feedback-linearization, *2009 IEEE International Conference on Mechatronics*, 2009.
- [38] Z. Shen, F. Li, X. Cao, and C. Guo, Prescribed performance dynamic surface control for trajectory tracking of quadrotor UAV with uncertainties and input constraints, *Int. J. Control.*, vol. 0, no. 0, pp. 121, 2020.
- [39] Z. Li, X. Ma, and Y. Li, Robust trajectory tracking control for a quadrotor subject to disturbances and model uncertainties, *Int. J. Syst. Sci.*, vol. 51, no. 5, pp. 839851, 2020.
- [40] S. Ahmed, H. Wang, and Y. Tian, Model-free control using time delay estimation and fractional-order nonsingular fast terminal sliding mode for uncertain lower-limb exoskeleton, *Journal of Vibration and Control*, vol. 24, no. 22, pp. 52735290, Jan. 2018.
- [41] I. Podlubny, "Fractional Differential Equations". New York: Academic, 1999.
- [42] S. Das, "Functional Fractional Calculus for System Identification and Controls". Heidelberg: Springer-Verlag, 2008.
- [43] Miller, Kenneth S., and B. Ross. "An Introduction to The Fractional Calculus and Fractional Differential Equations, John-Wiley and Sons." Inc. New York (1993).
- [44] S. Yu, X. Yu, B. Shirinzadeh, and Z. Man, Continuous finite-time control for robotic manipulators with terminal sliding mode, *Automatica*, vol. 41, no. 11, pp. 19571964, Nov. 2005.
- [45] G. V Raffo, M. G. Ortega, and F. R. Rubio, Automatica An integral predictive/nonlinear  $H_{\infty}$  control structure for a quadrotor helicopter, *Automatica*, vol. 46, no. 1, pp. 29-39, 2010.
- [46] F. P. Freire, N. A. Martins, and F. Splendor, A Simple Optimization Method for Tuning the Gains of PID Controllers for the Autopilot of Cessna 182 Aircraft Using Model-in-the-Loop Platform, *J. Control. Autom. Electr. Syst.*, vol. 29, no. 4, pp. 441450, 2018.
- [47] Y. Yu, X. A Ding, Quadrotor Test Bench for Six Degree of Freedom Flight, *Journal of Intelligent & Robotic Systems*, 68 (2012), pp. 323338.
- [48] X. Dong, et al., Time-Varying Formation Tracking for Second-Order Multi-Agent Systems Subjected to Switching Topologies With Application to Quadrotor Formation Flying, *IEEE Transactions on Industrial Electronics*, 64 (2017), pp. 50145024.



**Moussa Labbadi** received the B.S. and M.S. degrees in Mechatronic respectively from UAE of Tetouan and UH1 Faculty of Science and Technology of Settat, Morocco, in 2015 and 2017. He received his PhD at the E.3S of EMI, UM5 in Rabat, Morocco in Sep. 2020. He is currently a Post-Doc position at the MAScIR Foundation, Morocco. His research interests include Robotics, Aerial Robotics (Quadrotor UAV Drones), Mechatronics (Motion control smart machines), Estimation, Fractional-order control, Nonlinear control, sliding mode control and aerospace vehicles.